

# Dissolution Behavior of Lithium Oxide in Molten LiCl–KCl Systems

Yuya Kado,\* Takuya Goto, and Rika Hagiwara

Department of Fundamental Energy Science, Graduate School of Energy Science, Kyoto University, Yoshida-honmachi, Sakyo-ku, Kyoto 606-8501, Japan

The solubility of lithium oxide was measured in molten LiCl–KCl containing (58.5, 75, 90, and 100) mol % LiCl in the temperature range of (673 to 923) K. The melt with a higher content of LiCl has a higher solubility of Li<sub>2</sub>O. The pure LiCl has the highest solubility of Li<sub>2</sub>O, (12.0 ± 0.2) mol % at 923 K. The estimated standard formal potential of O<sub>2</sub>/O<sup>2-</sup> increases linearly as the temperature decreases and as the mole fraction of LiCl increases.

## Introduction

Electrochemical reduction processes in molten salts have been studied for metal refining and nuclear fuel reprocessing.<sup>1,2</sup> One of the most important achievements expected for the improvement of the efficiency of the process is the development of an inert anode. In our previous study, a boron-doped diamond (BDD) electrode was found to possess excellent properties for this purpose.<sup>3</sup> In addition to the electrode materials, high solubility of oxides in the melts is essential for fast electrochemical reduction of metal oxides with high efficiency.<sup>4</sup> Molten LiCl and CaCl<sub>2</sub> are strong candidates of the melts that satisfy the above requirement. Because of their high solubilities as oxides,<sup>2,5</sup> reduction of metal oxides has been achieved chemically and electrochemically in these melts.<sup>2,6</sup> However, the high melting temperatures of LiCl and CaCl<sub>2</sub> are disadvantageous for the process. Lower temperature operation has advantages such as lower corrosive and thermal damage to the vessels and electrode materials. Therefore, molten salts that have high solubilities as oxides at lower temperatures are indispensable for the reduction processes of metal oxides, although few reports are currently available on this subject. In this study, the temperature dependence of solubilities was investigated in molten LiCl–KCl systems with an electrochemical method. We selected the compositions of LiCl–KCl melts by referring to the reported binary phase diagram.<sup>7</sup>

## Experimental Section

A glassy carbon rod (Tokai Carbon) was used as an anode material for cyclic voltammetry. The cathode materials were also glassy carbon rods at temperatures higher than 823 K, whereas aluminum plates (99.2 %, Nilako) were used at temperatures lower than 823 K. The reference electrode was an Ag<sup>+</sup>/Ag electrode. A silver wire (99.99 %, Japan Metal Service) was immersed in the LiCl–KCl melt of each composition containing 0.5 mol % AgCl (99.5 %, Wako Pure Chemical), which was set in a Pyrex glass or mullite tube. The potential of the reference electrode was standardized against the Li<sup>+</sup>/Li. A nickel wire was used as a current collector and was immersed in molten lithium metal to measure the potential of Li<sup>+</sup>/Li against Ag<sup>+</sup>/Ag.

Reagent grade LiCl (Aldrich-APL, 99.99 %), KCl (Aldrich-APL, 99.99 %), and a eutectic mixture of LiCl–KCl (Aldrich-

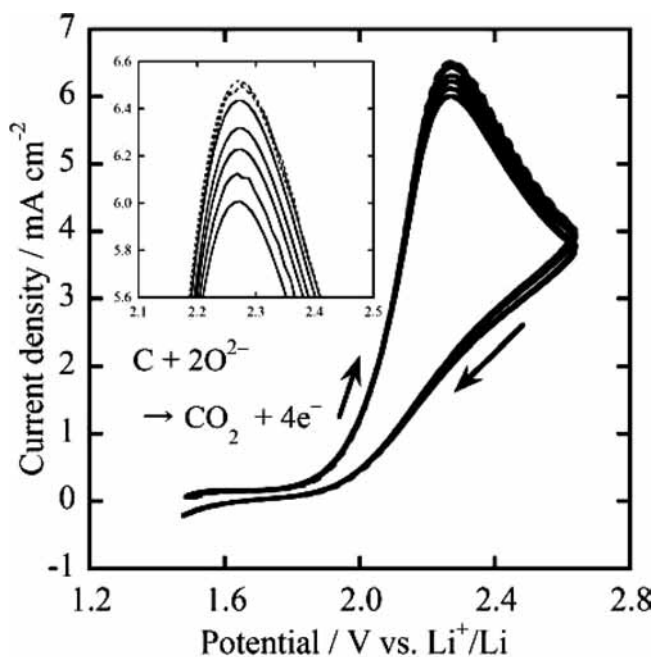


**Figure 1.** Cyclic voltammograms of a glassy carbon rod in eutectic LiCl–KCl (58.5:41.5) with the addition of Li<sub>2</sub>O (solid line, (0.975, 1.000, 1.025, 1.050, and 1.100) mol %; dotted line, (1.150, 1.200, and 1.225) mol %) at 773 K. Scan rate is 0.2 V·s<sup>-1</sup>. The inset is the close-up drawing around the current density peaks.

APL, 99.98 %) were used for the melt. The solubility of lithium oxide (Li<sub>2</sub>O, Aldrich, 97 %) was measured in LiCl and LiCl–KCl mixtures of following compositions: LiCl:KCl = 90:10, 75:25, 58.5:41.5 (eutectic). The experimental temperature range was (673 to 923) K. All experiments were conducted in a glove box filled with Ar gas dried and deoxygenated by a gas purifier (MIWA, MS3-H60SN). The concentration of water and oxygen gas in the atmosphere were kept at less than 1 ppm.

Electrochemical measurements were performed using an electrochemical measurement system (HZ-3000, Hokuto Denko).

## Results and Discussion

**Temperature Dependence of the Solubility of Lithium Oxide in Molten LiCl–KCl.** Figure 1 shows the cyclic volta-

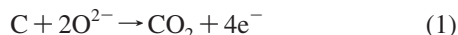
\* Corresponding author. E-mail: yuuya-kado@t02.mbox.media.kyoto-u.ac.jp.

**Table 1. Temperature Dependence of the Solubility Products of Li<sub>2</sub>O in Molten LiCl–KCl Systems<sup>a</sup>**

LiCl:KCl	T/K	ln $K_{sp}$
100:0	873 to 923	$-(2.44 \pm 0.47) \cdot 10^3 T^{-1} + 0.52 \pm 0.01$
90:10	823 to 923	$-(0.41 \pm 0.14) \cdot 10^3 T^{-1} - 2.17 \pm 0.01$
75:25	773 to 873	$-(1.79 \pm 0.35) \cdot 10^3 T^{-1} - 1.46 \pm 0.03$
58.5:41.5	673 to 823	$-(2.39 \pm 0.29) \cdot 10^3 T^{-1} - 2.43 \pm 0.03$

<sup>a</sup> Error values are the 95 % confidence intervals.

mmogram in the positive potential region obtained in a eutectic LiCl–KCl (58.5:41.5) melt containing various amounts of Li<sub>2</sub>O at 773 K using a glassy carbon rod electrode. A sharp increase in anodic currents was observed at about 2.0 V (vs Li<sup>+</sup>/Li). This current is attributed to the evolution of carbon dioxide.<sup>8</sup>



The peak currents corresponding to CO<sub>2</sub> evolution plotted against the amount of Li<sub>2</sub>O added to the melt are shown in Figure 2. The current increased almost linearly as the amount of Li<sub>2</sub>O added increased and finally showed a constant value when the melt was saturated with Li<sub>2</sub>O. As a result, the solubility of Li<sub>2</sub>O in eutectic LiCl–KCl at 773 K was determined to be 1.12 mol %. The intersecting point of the two lines shown in the Figure was chosen to be a saturation point. In the same manner, the solubilities of Li<sub>2</sub>O were determined at (673, 723, 773, and 823) K. They were (0.708 ± 0.055, 0.966 ± 0.031, 1.14 ± 0.05, and 1.32 ± 0.53) mol %, respectively. The error value denotes the 95 % confidence interval. The solubility of Li<sub>2</sub>O was also determined in the pure LiCl and LiCl–KCl mixtures; LiCl:KCl = 90:10 and 75:25. The results are summarized in Figures 3 and 4. The temperature dependence of the solubility product,  $K_{sp}$ , is given by the empirical equations in Table 1, where  $T$  is the absolute temperature.  $K_{sp}$  is determined from eq 2 by using the mole fraction of lithium ion,  $X_{Li^+}$ , and that of the oxide ion,  $X_{O^{2-}}$ . The solubility of Li<sub>2</sub>O increases with an elevation of the temperature of the melt and an increase in the mole fraction of LiCl in the melt.

$$K_{sp} = X_{Li^+}^2 \cdot X_{O^{2-}} \quad (2)$$

**Thermodynamical Study on the Standard Formal Potential of O<sub>2</sub>/O<sup>2-</sup>.** The standard formal potential of O<sub>2</sub>/O<sup>2-</sup>,  $E_{O_2/O^{2-}}^0$ , was calculated and estimated from the results obtained from the measurement of the solubility. The oxygen electrode reaction and the Nernstian equation in molten salts are described as follows



$$E_{O_2/O^{2-}} = E_{O_2/O^{2-}}^0 + \frac{RT}{2F} \ln \frac{f_{O_2}}{a_{O^{2-}}} \quad (4)$$

where  $R$  is the gas constant,  $F$  is the Faraday constant,  $f_{O_2}$  is the fugacity of O<sub>2</sub>,  $a_{O^{2-}}$  is the activity of O<sup>2-</sup>, and  $E_{O_2/O^{2-}}^0$  is

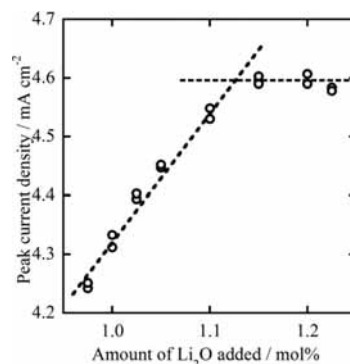


**Figure 2.** Peak currents against the amount of Li<sub>2</sub>O added to the melt determined from cyclic voltammograms of a glassy carbon electrode in eutectic LiCl–KCl (58.5:41.5) at 773 K.

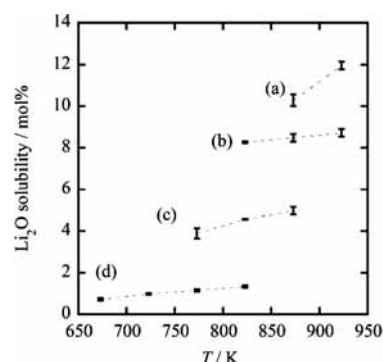


**Figure 3.** Solubilities of Li<sub>2</sub>O in molten LiCl–KCl systems. LiCl:KCl = (a) 100:0, (b) 90:10, (c) 75:25, and (d) 58.5:41.5.

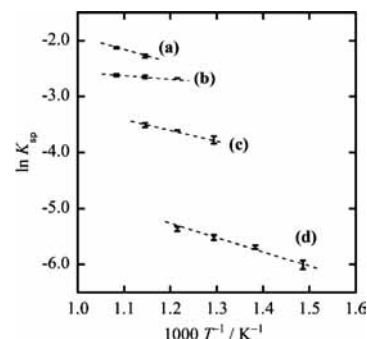


**Figure 4.** Relationship between temperature and the solubility products of Li<sub>2</sub>O in molten LiCl–KCl systems. LiCl:KCl = (a) 100:0, (b) 90:10, (c) 75:25, and (d) 58.5:41.5.

the standard potential of O<sub>2</sub>/O<sup>2-</sup>. Equation 4 is described below using the fugacity coefficient of O<sub>2</sub> ( $\gamma_{O_2}$ ), the activity coefficient of the O<sup>2-</sup> anion ( $\gamma_{O^{2-}}$ ), and the pressure of O<sub>2</sub> ( $P_{O_2}$ )

$$E_{O_2/O^{2-}} = E_{O_2/O^{2-}}^0 + \frac{RT}{2F} \ln \frac{(\gamma_{O_2} P_{O_2})^{1/2}}{(\gamma_{O^{2-}})(X_{O^{2-}})} \quad (5)$$

Consequently,  $E_{O_2/O^{2-}}^0$  is given by the equation

**Table 2. Thermodynamic Data for Equation 14: 2Li(l) + 1/2O<sub>2</sub>(g) → 2Li<sup>+</sup> + O<sup>2-</sup><sup>a</sup>**

LiCl:KCl	T	$\Delta G^0$ (13)	$\Delta S^0$ (13)	$\Delta H^0$ (13)
	K	kJ·mol <sup>-1</sup>	J·mol <sup>-1</sup> ·K <sup>-1</sup>	kJ·mol <sup>-1</sup>
100:0	873 to 923	$(-586.9 \pm 0.1) + (137 \pm 4) \cdot 10^{-3}T$	-137 ± 4	-586.9 ± 0.1
90:10	823 to 923	$(-602.7 \pm 0.1) + (158 \pm 1) \cdot 10^{-3}T$	-158 ± 1	-602.7 ± 0.1
75:25	773 to 873	$(-591.4 \pm 0.2) + (152 \pm 4) \cdot 10^{-3}T$	-152 ± 4	-591.4 ± 0.2
58.5:41.5	673 to 823	$(-586.5 \pm 0.2) + (160 \pm 3) \cdot 10^{-3}T$	-160 ± 3	-586.5 ± 0.2

<sup>a</sup> Error values are the 95 % confidence intervals.

$$E_{\text{O}_2/\text{O}^{2-}}^0 = E_{\text{O}_2/\text{O}^{2-}}^{0'} + \frac{RT}{2F} \ln \frac{P_{\text{O}_2}^{1/2}}{X_{\text{O}^{2-}}} \quad (6)$$

where  $E_{\text{O}_2/\text{O}^{2-}}^{0'}$  is the standard formal potential of  $\text{O}_2/\text{O}^{2-}$  which is given by the following equation

$$E_{\text{O}_2/\text{O}^{2-}}^{0'} = E_{\text{O}_2/\text{O}^{2-}}^0 + \frac{RT}{2F} \ln \frac{\gamma_{\text{O}_2}^{1/2}}{\gamma_{\text{O}^{2-}}} \quad (7)$$

The solution equilibrium of  $\text{Li}_2\text{O}$  is described by eq 8, and the free energy change is given by eq 9. When a  $\text{LiCl-KCl}$  melt is saturated with  $\text{Li}_2\text{O}$ , the solution equilibrium is achieved and the free energy change of eq 8 is zero. Therefore, the standard free energy change of eq 8,  $\Delta G^0$  (8), can be shown by eq 10 using the activity of the  $\text{Li}^+$  cation,  $a_{\text{Li}^+}$



$$\Delta G(8) = \Delta G^0(8) - RT \ln(a_{\text{Li}^+}^2 \cdot a_{\text{O}^{2-}}) \quad (9)$$

$$\Delta G^0(8) = RT \ln(a_{\text{Li}^+}^2 \cdot a_{\text{O}^{2-}}) \quad (10)$$

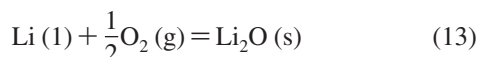
Here we introduce the standard formal free energy,  $\Delta G^{0'}$  (8), described by the equation

$$\Delta G^{0'}(8) = \Delta G^0(8) - RT \ln(\gamma_{\text{Li}^+}^2 \cdot \gamma_{\text{O}^{2-}}) \quad (11)$$

where  $\gamma_{\text{Li}^+}$  is the activity coefficient of the  $\text{Li}^+$  cation.<sup>9</sup> Therefore,  $\Delta G^{0'}$  (8) is given by the following equation using the mole fraction of the  $\text{Li}^+$  cation

$$\Delta G^{0'}(8) = RT \ln(X_{\text{Li}^+}^2 \cdot X_{\text{O}^{2-}}) \quad (12)$$

This concept is similar to that of the standard formal potential in eq 7. Also, the standard formal free energy of the following reaction,  $\Delta G^{0'}$  (13), is available from reported thermodynamical data.<sup>10</sup>



The free energy of the reaction shown in eq 14,  $\Delta G^{0'}$  (14), is calculated using  $\Delta G^{0'}$  (8) and  $\Delta G^{0'}$  (13).

**Table 3. Standard Formal Potential of  $\text{O}_2/\text{O}^{2-}$  in Molten  $\text{LiCl-KCl}$  Systems<sup>a</sup>**

LiCl:KCl	T/K	$E_{\text{O}_2/\text{O}^{2-}}^{0'}/\text{V}$ vs $\text{Li}^+/\text{Li}$
100:0	873 to 923	$(-7.08 \pm 0.24) \cdot 10^{-4}T + (3.042 \pm 0.001)$
90:10	823 to 923	$(-8.11 \pm 0.10) \cdot 10^{-4}T + (3.124 \pm 0.001)$
75:25	773 to 873	$(-7.70 \pm 0.21) \cdot 10^{-4}T + (3.078 \pm 0.001)$
58.5:41.5	673 to 823	$(-7.90 \pm 0.16) \cdot 10^{-4}T + (3.042 \pm 0.001)$

<sup>a</sup> Error values are the 95 % confidence intervals.

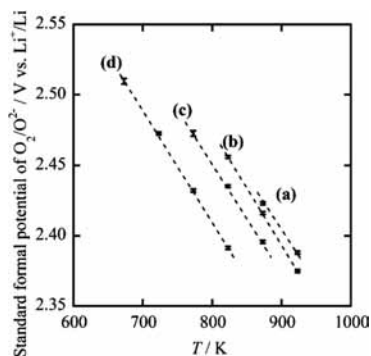
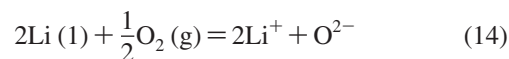


**Figure 5.** The standard formal potential of  $\text{O}_2/\text{O}^{2-}$  in molten  $\text{LiCl-KCl}$  systems. LiCl:KCl = (a) 100:0, (b) 90:10, (c) 75:25, and (d) 58.5:41.5.



$$\Delta G^{0'}(14) = \Delta G^{0'}(13) - \Delta G^{0'}(8) \quad (15)$$

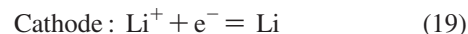
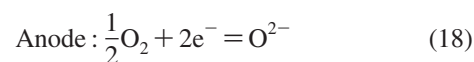
$\Delta G^{0'}$  (14) is therefore obtained from experimental data of  $\Delta G^{0'}$  (8). In addition, the standard formal entropy of formation,  $\Delta S^{0'}$  (14), and the standard formal enthalpy of formation,  $\Delta H^{0'}$  (14), are calculated according to eqs 16 and 17

$$\Delta S^{0'}(14) = -\left(\frac{\partial \Delta G^{0'}(14)}{\partial T}\right)_p \quad (16)$$

$$\Delta H^{0'}(14) = \Delta G^{0'}(14) + T\Delta S^{0'}(14) \quad (17)$$

The obtained formal thermodynamic quantities are shown in Table 2. The error values are the 95 % confidence intervals. Table 2 shows that  $\Delta H^{0'}$  (14) is almost constant in all systems. However,  $\Delta S^{0'}$  (14) obtained in the pure  $\text{LiCl}$  is remarkably different from that in the melt containing  $\text{KCl}$ , which is attributed to the difference in the structure of the oxide ion in the melts.

Equation 14 is divided into the following two half-equations



Therefore, the standard free energy of eq 14 is given by the equation

$$\Delta G^0(14) = -2F(E_{\text{O}_2/\text{O}^{2-}}^0 - E_{\text{Li}^+/\text{Li}}^0) \quad (20)$$

where  $E_{\text{Li}^+/\text{Li}}^0$  is the standard potential of  $\text{Li}^+/\text{Li}$ . However, those values cannot be experimentally measured. Here standard formal free energy,  $\Delta G^{0'}$  (14), is expressed by eq 21<sup>9</sup>

$$\Delta G^{0'}(14) = \Delta G^0(14) - RT \ln \frac{\gamma_{\text{O}_2}^{1/2}}{\gamma_{\text{O}^{2-}} \cdot \gamma_{\text{Li}^+}^2} \quad (21)$$

Therefore,  $\Delta G^{0'}$  (14) is given by the equation

$$\Delta G^{0'}(14) = -2F(E_{\text{O}_2/\text{O}^{2-}}^{0'} - E_{\text{Li}^+/\text{Li}}^{0'}) \quad (22)$$

where  $E_{\text{Li}^+/\text{Li}}^{0'}$  is the standard formal potential of  $\text{Li}^+/\text{Li}$ , which is given by the following equation

$$\begin{aligned} E_{\text{Li}^+/\text{Li}}^{0'} &= E_{\text{Li}^+/\text{Li}} - \frac{RT}{F} \ln X_{\text{Li}^+} \\ &= -\frac{RT}{F} \ln X_{\text{Li}^+} \end{aligned} \quad (23)$$

$E_{\text{Li}^+/\text{Li}}$  is defined to be zero in this study.

Consequently, the standard formal potential of  $\text{O}_2/\text{O}^{2-}$ ,  $E_{\text{O}_2/\text{O}^{2-}}^{0'}$  (vs  $\text{Li}^+/\text{Li}$ ) is obtained by using eqs 12, 15, 22, and 23. Here the solubility of  $\text{Li}_2\text{O}$  was used as the mole fraction of the oxide ion,  $X_{\text{O}^{2-}}$ . The result obtained in each  $\text{LiCl-KCl}$  melt is shown in Table 3 and Figure 5. The standard formal potential of  $\text{O}_2/\text{O}^{2-}$  increases with a decrease in temperature and an increase in the mole fraction of  $\text{LiCl}$  in the melt.

## Conclusions

The solubilities of  $\text{Li}_2\text{O}$  in molten  $\text{LiCl-KCl}$  systems were determined in the temperature range of (673 to 923) K. The melt with a higher content of  $\text{LiCl}$  in molten  $\text{LiCl-KCl}$  systems has a higher solubility of  $\text{Li}_2\text{O}$ . The pure  $\text{LiCl}$  has the highest solubility of  $\text{Li}_2\text{O}$ ,  $(12.0 \pm 0.2)$  mol % at 923 K.

The standard formal potential of  $O_2/O^{2-}$  evaluated from the results in the present study increases linearly with a decrease in temperature and an increase in the mole fraction of LiCl in the melt.

#### Supporting Information Available:

Data for Figures 3, 4, and 5. This material is available free of charge via the Internet at <http://pubs.acs.org>.

#### Literature Cited

- (1) Chen, G. Z.; Fray, D. J.; Farthing, T. W. Direct electrochemical reduction of titanium dioxide to titanium in molten calcium chloride. *Nature* **2000**, *407*, 361–364.
- (2) Usami, T.; Kurata, M.; Inoue, T.; Sims, H. E.; Beetham, S. A.; Jenkins, J. A. Pyrochemical reduction of uranium dioxide and plutonium dioxide by lithium metal. *J. Nucl. Mater.* **2002**, *300*, 15–26.
- (3) Goto, T.; Araki, Y.; Hagiwara, R. Oxygen gas evolution on boron-doped diamond electrode in molten chloride systems. *Electrochem. Solid-State Lett.* **2006**, *9*, D5–D7.
- (4) Sakamura, Y.; Kurata, M.; Inoue, T. Electrochemical reduction of  $UO_2$  in molten LiCl and LiCl–KCl eutectic. *Proc. Int. Symp. Molten Salt Chem. Technol.*, 7th **2005**, *2*, 597–601.
- (5) Levin, E. M.; Robbins, C. R.; McMurdie, H. F. Phase Diagrams for Ceramists: 1969 Supplement; American Ceramic Society: Columbus, OH, 1969.
- (6) Yasuda, K.; Nohira, T.; Amezawa, K.; Ogata, Y. H.; Ito, Y. Mechanism of direct electrolytic reduction of solid  $SiO_2$  to Si in molten  $CaCl_2$ . *J. Electrochem. Soc.* **2005**, *152*, D69–D74.
- (7) Levin, E. M.; Robbins, C. R.; McMurdie, H. F. Phase Diagrams for Ceramists; American Ceramic Society: Columbus, OH, 1964.
- (8) Sakamura, Y.; Kurata, M.; Inoue, T. Electrochemical Reduction of  $UO_2$  in Molten  $CaCl_2$  or LiCl. *J. Electrochem. Soc.* **2006**, *153*, D31–D39.
- (9) Nakajima, H.; Nohira, T.; Ito, Y. Thermodynamic investigations of a hydrogen electrode reaction in a molten LiCl–KCl–LiH system. *Electrochem. Solid-State Lett.* **2002**, *5*, E17–E20.
- (10) Facility for the Analysis of Chemical Thermodynamics (FACT) Home Page. <http://www.crct.polymtl.ca/fact/>, CRCT, 1996.

Received for review July 11, 2008. Accepted October 5, 2008.

JE800540C